BBA - Molecular Basis of Disease 1865 (2019) 1138–1151

Contents lists available at ScienceDirect

BBA - Molecular Basis of Disease

journal homepage: www.elsevier.com/locate/bbadis

Dystrophic *mdx* mouse myoblasts exhibit elevated ATP/UTP-evoked metabotropic purinergic responses and alterations in calcium signalling

Justyna Róg[a,d], Aleksandra Oksiejuk[a], Maxime R.F. Gosselin[b], Wojciech Brutkowski[a], Dorota Dymkowska[a], Natalia Nowak[c], Samuel Robson[b], Dariusz C. Górecki[b,d,*,1], Krzysztof Zabłocki[a,**,1]

[a] Laboratory of Cellular Metabolism, Nencki Institute of Experimental Biology, Polish Academy of Sciences, Warsaw, Poland
[b] School of Pharmacy and Biomedical Sciences, University of Portsmouth, Portsmouth, UK
[c] Laboratory of Imaging Tissue Structure and Function, Neurobiology Center Nencki Institute of Experimental Biology of the Polish Academy of Sciences, Warsaw, Poland
[d] Military Institute of Hygiene and Epidemiology, Warsaw, Poland

ARTICLE INFO

Keywords:
Calcium homeostasis
Duchenne muscular dystrophy
Myoblast
P2Y receptors

ABSTRACT

Pathophysiology of Duchenne Muscular Dystrophy (DMD) is still elusive. Although progressive wasting of muscle fibres is a cause of muscle deterioration, there is a growing body of evidence that the triggering effects of DMD mutation are present at the earlier stage of muscle development and affect myogenic cells. Among these abnormalities, elevated activity of P2X7 receptors and increased store-operated calcium entry myoblasts have been identified in *mdx* mouse. Here, the metabotropic extracellular ATP/UTP-evoked response has been investigated. Sensitivity to antagonist, effect of gene silencing and cellular localization studies linked these elevated purinergic responses to the increased expression of P2Y2 but not P2Y4 receptors. These alterations have physiological implications as shown by reduced motility of *mdx* myoblasts upon treatment with P2Y2 agonist. However, the ultimate increase in intracellular calcium in dystrophic cells reflected complex alterations of calcium homeostasis identified in the RNA seq data and with significant modulation confirmed at the protein level, including a decrease of Gq11 subunit α, plasma membrane calcium ATP-ase, inositol-2,4,5-trisphosphate-receptor proteins and elevation of phospholipase Cβ, sarco-endoplamatic reticulum calcium ATP-ase and sodium-calcium exchanger. In conclusion, whereas specificity of dystrophic myoblast excitation by extracellular nucleotides is determined by particular receptor overexpression, the intensity of such altered response depends on relative activities of downstream calcium regulators that are also affected by *Dmd* mutations. Furthermore, these phenotypic effects of DMD emerge as early as in undifferentiated muscle. Therefore, the pathogenesis of DMD and the relevance of current therapeutic approaches may need re-evaluation.

1. Introduction

Duchenne muscular dystrophy (DMD) is a lethal inherited disorder causing severe progressive muscle loss with sterile inflammation accompanied by cognitive and behavioural impairments and decreased bone strength. The disease is caused by the lack of dystrophin due to out-of-frame mutations in the *DMD* gene and the diversity of symptoms illustrates the importance of dystrophin in a range of cells. Indeed, *DMD* is the largest human gene known with 79 exons encoding 3 full-length (427 kDa) expressed in temporally-controlled and tissue-specific manners in muscle but also in non-muscle cells. The five progressively-shortened isoforms (Dp412, Dp260, Dp140, Dp116 and Dp71) also present specific spatio-temporal patterns of expression, occurring as early as in embryonic stem cells and they have distinct roles, which are only partially understood [1]. Therefore, *DMD* is a multi-functional gene with a complex spatio-temporal expression pattern. Yet, since the

Abbreviations: $[Ca^{2+}]c$, cytosolic Ca^{2+} concentration; DMD, Duchenne Muscle Dystrophy; eATP, extracellular ATP; NCX, sodium-calcium exchanger; PLCβ, phospholipase Cβ; PMCA, plasma membrane calcium ATP-ase; SERCA, sarco-endoplasmic reticulum calcium ATP-ase

* Correspondence to: D.C. Górecki, School of Pharmacy and Biomedical Sciences, University of Portsmouth, St Michael's Building, White Swan Road, Portsmouth PO1 2DT, UK.
** Correspondence to: K. Zabłocki, Nencki Institute of Experimental Biology, 3 Pasteura Str., 02-093 Warsaw, Poland.
E-mail addresses: darek.gorecki@port.ac.uk (D.C. Górecki), k.zablocki@nencki.gov.pl (K. Zabłocki).
[1] Senior co-authors (equal contribution).

https://doi.org/10.1016/j.bbadis.2019.01.002
Received 7 September 2018; Received in revised form 14 December 2018; Accepted 2 January 2019
Available online 24 January 2019
0925-4439/

life-threatening effects of *DMD* mutations present in striated muscles, investigations have focused on the full-size dystrophins, which have been attributed with the key role in protecting myofibres. Dystrophin there localizes to the cytoplasmic face of the sarcolemma where it anchors a set of dystrophin-associated proteins (DAP) tethering this complex to the intracellular cytoskeleton and extracellular matrix proteins [2]. The current understanding is that the dystrophin-DAP complex provides structural stability to the myofibre sarcolemma and its loss triggers muscle degeneration by destabilization of this membrane, allows extracellular Ca^{2+} influx leading to abnormal intracellular calcium signalling and a downstream cascade eventually resulting in muscle cell death. The evidence for this mechanical/structural instability triggering this complex train of pathological events is that the re-expression of dystrophin improves structure and function of dystrophic muscles. However, this does not necessarily prove that the disease starts with the absence of dystrophin in myofibres. Indeed, RNAi mediated knock-down of the full-length dystrophin expression in adult mouse did not trigger muscle degeneration despite a loss of protein from the sarcolemma [3]. Furthermore, the knockout of the DAP protein dystroglycan in mature muscle was associated with loss of dystrophin from the sarcolemma but caused no necrosis or sarcolemmal fragility [4]. These results indicate a need for critical re-evaluation of current views regarding the pathogenesis of DMD and the therapeutic strategies being developed [5]. It is important to consider whether the absence of dystrophin in fully differentiated muscle fibres is the mechanism of disease and therefore, whether dystrophin re-expression in myofibres would cure this disease. Indeed, dystrophin is expressed early in embryogenesis (mouse E9.5) and its absence in *mdx* mouse severely disrupts muscle development due to stem cell loss and disrupted muscle patterning [6]. The absence of DMD gene expression also affects stem cells leading to the intrinsic exhaustion of stem cells pool thus compromising muscle regeneration [7,8]. This abnormality has been linked to the absence of the full-length dystrophin in activated satellite cells, where it regulates cell polarity and reduced number of myogenic progenitors [9]. A recent study linked the DAP in muscle stem cells undergoing asymmetric division with epigenetic activation [10]. Furthermore, myogenic cells from both Duchenne patients [11,12] and *mdx* mice [13] show abnormalities of a range of important functions including altered proliferation and differentiation and defects of energy metabolism with disorganized mitochondrial networks [14]. Moreover, a purinergic phenotype involving an increased expression and activity of P2X7 receptors has been identified in myoblasts of the *mdx* mouse model of Duchenne type muscular dystrophy [15,16] as well as in human DMD lymphoblasts [17]. Further analyses led to the discovery of a novel mechanism of P2RX7-evoked autophagic death in dystrophic muscle [18]. Finally, ablation or pharmacological inhibition of P2RX7 significantly reduced the disease progression in the *mdx* model of DMD [19–21].

Besides the aberrant ionotropic response to extracellular ATP, we have also found increased activity of store-operated calcium entry mechanisms in dystrophic myoblasts [22]. These and other studies demonstrate that abnormalities of calcium homeostasis in DMD occur in myoblasts and not only in fully differentiated myofibres and that they involve alterations of specific cellular mechanisms rather than mechanical membrane instability.

Indeed, here we have presented evidence of a profound alteration of calcium homeostasis in myoblasts with the mutant *Dmd* gene, which involves the metabotropic response to eATP, which, in vivo, is released at high levels from damaged muscles. This purinergic phenotype is combined with dysregulation of the intracellular calcium machinery. Altogether, substantially increased activity of P2RY2 was identified in dystrophic mouse myoblasts stimulated with ATP or UTP. While this effect could be attributed to the increased P2RY2 levels in the plasma membrane, the specificity of calcium responses in *mdx* myoblasts extends beyond the stimulation of P2RY2. The height and shape of elevated calcium transients reflect the combination of both the increased receptor activity and other significantly altered proteins involved in calcium signalling regulation in these cells.

2. Material and methods

2.1. Cell culture

Immortalized *mdx* mouse and dystrophin-positive control (w/t) myoblasts were used. These two cell lines were of the same genetic background, as the two mouse strains from which the cells were derived originated from the same parental inbred mouse strain H2Kb-tsA58 ("immorto mouse"), expressing the SV40 large T antigen gene with the tsA58 mutation. The H2Kb-tsA58 mdx strain was established by crossing male mouse homozygous for H2Kb-tsA58 with female *mdx* mice [23]. *Mdx* and w/t cells used here are highly homogenous populations differing only in the presence or absence of a point mutation in the dystrophin gene exhibiting muscle phenotype and myogenic potential following differentiation [16,24–26]. Cells were cultured in Dulbecco's modified Eagle's medium (DMEM, Sigma Chemical Company, St. Louis, MO, USA) supplemented with 20% foetal calf serum, 4 mM L-glutamine, 100 unit/ml penicillin, 100 μg/ml streptomycin, and 20 unit/ml murine γ-interferon (Invitrogen, San Diego, CA, USA) at 33 °C. Under such conditions a differentiation of these cells was efficiently prevented. Moreover both cell lines were also cultured at 37 °C in absence of γ-interferon in KnockOut DMEM (Invitrogen) supplemented with 10% v/v KSR (Knockout Serum Replacement, Invitrogen), 5% v/v DHS (Donor Horse Serum, Sera Labs) and 2 mM L-glutamine. Under these conditions the cells exhibit properties of primary-like ("de-immortalized") cells because of the loss of expression and thermal degradation of the immortalisation factor.

2.2. RNAseq

Immortalized myoblast cell lines were cultured in immorto conditions to produce 4 populations of each genotype growing apart for 2 passages and then re-plated and cultured for 48 h in primary myoblast conditions at 37 °C with 5% CO_2 in IFN-γ free medium (see above). Total RNA was extracted using an RNEasy plus universal mini kit (QIAGEN 73404) following manufacturer's instructions. Briefly, cells were washed 3 times with warm DPBS before being lysed directly on the culture plate by adding QIAZOL lysing buffer and using a cell scraper to disrupt the cells. Samples were then treated as per provided protocol. After extraction, total RNA samples were sent to THERAGEN ETEX (Republic of Korea) for quality control and sequencing. Quality was assessed using an Agilent Bioanalyzer 2100, with a minimum RNA integrity number (RIN) of 7.0 or greater being required. Libraries were prepared using an Illumina TruSeq stranded total RNA kit, including ribodepletion using the Ribo-Zero Human/Mouse/Rat kit to remove ribosomal RNA. Libraries were sequenced in a paired-end 100 bp run using an Illumina HiSeq 2500 sequencing platform.

Quality control of raw fast reads was conducted using fastQC [27]. Reads were trimmed using trim-galore [28] with parameters-to remove adapter sequence and low quality sequence tails. Trimmed reads were mapped against the GRCm38 *Mus musculus* genome from Ensembl using the STAR universal RNA seq aligner [29] with parameters '"–outSAMmultNmax 300 –outSAMstrandField intronMotif'.

Differential expression analysis was conducted using the DESeq2 package [30] in R [31]. Gene models were taken from Ensembl version 91, and read counts over unique genes were quantified using the *summarizeOverlaps()* function in the GenomicAlignments package [32] using parameters 'mode = "Union", singleEnd = FALSE, ignore.strand = FALSE, fragments = FALSE, preprocess.reads = invertStrand'. *P* values were adjusted for multiple testing by using the Benjamini and Hochberg correction [33]. Significantly differentially expressed genes were identified based on a fold-change of 2-fold or greater (up- or downregulated) and an adjusted *p*-value < 0.05. An additional filter was put in place to remove genes where

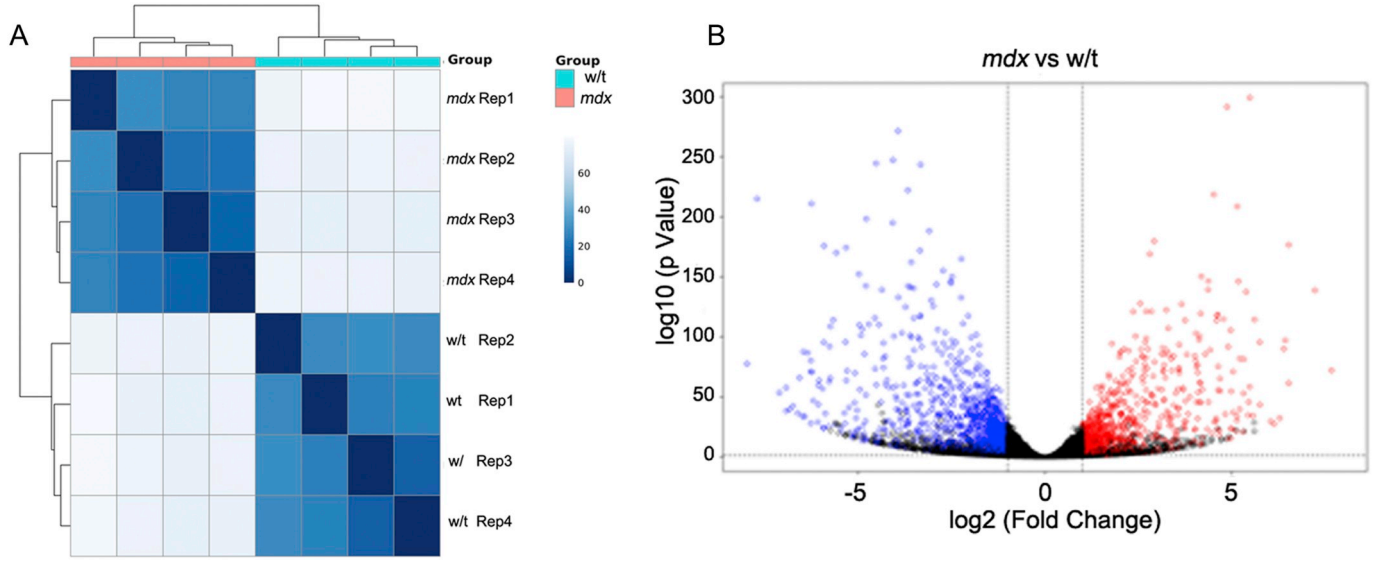

Fig. 1. RNAseq analysis in myoblasts derived from w/t and mdx mice.
A: Hierarchical clustering of the normalised read counts across all genes identifies clear discrimination between the dystrophic (mdx) and control (w/t) cells. Cell colour represents the dissimilarity between samples, with dark blue indicating no difference.
B: Volcano plot showing the results of the differential expression analyses across all genes, with the (-log10) adjusted *p* value on the y-axis representing the significance of the change, and the log2 fold change on the x-axis representing the magnitude of the change. Genes are classed as showing significant differential expression with fold change > 2-fold (up or down) with an adjusted *p*-value < 0.05. In addition, the expression must show FPKM > 1 in at least one of the two conditions. Significantly upregulated (red) and downregulated (blue) genes between the mdx (SC5) and control (IMO) cells are highlighted.

the mean normalised FPKM (fragments per kilobase mapped) was < 1 for both conditions to avoid changes in low abundance transcripts. Gene ontology analysis was conducted using the clusterProfiler package [34].

2.3. RNA extraction, reverse transcription and quantitative RT-PCR

Total RNA was isolated using Trizol method (TRI reagent, T9424; Sigma). The quality and quantity of samples were determined using a NanoDrop spectrophotometer. Only RNA with an absorbance ratio 260/280 between 1.8 and 2.0 was used to reverse transcription. Complementary DNA (cDNA) was synthesized from 2 μg of total RNA using First Strand cDNA Synthesis Kit with M-MLV reverse transcriptase and oligo(dT) primers (#K1612, Thermo Fischer Scientific), according to the manufacturer's instructions.

RT-qPCR was performed using TaqMan Fast Universal PCR Master Mix (4,352,042, Applied Biosystems) and TaqMan Gene Expression Assays (the primers ID: Mm 01274119_m1 for P2RY2, Mm 00445136_s1 for P2RY4) on the 7500 ABI Prism Real-Time PCR System (Applied Biosystems). The level of expression of target genes were normalised to the expression of GAPDH (primer ID: Mm99999915_g1) housekeeping gene. Analysis of relative gene expression data were determined by 2-ΔΔCt method using StepOne Software.

2.4. Cell lysis, protein extraction and analysis

Proteins were extracted from adherent cells by scraping into extraction buffer (1× LysisM, 1× protease inhibitor cocktail, 2 x phosphatase inhibitor cocktail (all Roche), 2 mM sodium orthovanadate (Sigma) suspending with the use of automatic pipets followed by repeatedly forcing through the syringe needle (0.5 mm in diameter) and incubation of the suspension on ice for 20 min. After centrifugation (15,000 ×*g*, for 20 min at 4 °C) protein concentrations in supernatants collected were determined using a Bradford protein assay (Bio-Rad). Remaining supernatants were mixed with sample buffer at 3:1 $^{v}/_{v}$ ratio, heated for 5 min at 95 °C and chilled on ice and stored at −20 °C. Proteins (20 μg of each sample) were separated on 0.1% SDS-polyacrylamide gels (6–12% $^{w}/_{v}$ depending on the molecular mass of protein) and electroblotted onto Immobilon-PVDF Transfer Membrane (Merck Millipore). Blots were blocked in 5% $^{w}/_{v}$ non-fat milk or 5% BSA (Albumin, Bovine Serum, 12659, Merck Millipore) powder solved in 1 × TBST, 0.01% $^{v}/_{v}$ Tween-20 (Sigma) for 1 h at room temperature (RT) prior to probing with appropriate primary antibody diluted in a blocking buffer containing 2.5% milk or 5% BSA (incubated overnight at 4 °C with agitation). To identify proteins of interest following primary antibodies were applied: P2RY2 (1:270, APR-10) and P2RY4 (1:300, APR-006; all Alomone Labs), calsequestrin (ab126241), calreticulin (ab128885), SERCA1 (ab124501) and SERCA2 (ab91032; all diluted 1:1000, Abcam), Gαq11 (1:1000, 06-709 Merck Millipore), PLCβ isoforms 1-4 (sc-5291, sc-515912, sc-133231, sc-166131, respectively; all diluted 1:100, Santa Cruz Biotechnology), NCX1 (1:1000, R3F1 Swant) and NCX3 (1:500, ab84708 Abcam) and IP3R (diluted 1:1000 in BSA solution as described above, #8568 Cell Signalling Technology). Then membranes were washed (3×) with 1 × PBST for 10 min each wash and incubated with anti-Rabbit (diluted 1:5000, ab6721, Abcam) or anti-Mouse (1:3000, ab6728, Abcam) horseradish peroxidase-conjugated secondary antibody for 1 h at RT.

Specific protein bands were visualized using luminol-based substrates (Millipore) and images obtained using a Fusion FX (Vilber Lourmat). β-tubulin (1:10000, ab21058), Na+-K+ ATPase (1:200, ab7671) and caveolin (1:2000, ab2910; all Abcam) antibodies were used as a protein-loading control dependent on the protocol. Densitometric analyses of specific protein bands were made using exposure times within the linear range and the integrated density measurement function of BIO-1D (Vilber Lourmat). All experiments were repeated at least 3 times with similar results obtained in each replicate.

2.5. siRNA transfection

P2RY2 gene silencing was performed with the use of short interfering RNA (Silencer Select Pre-designed siRNA ID #s71197, Invitrogen, Thermo Fisher Scientific. Scrambled siRNA oligonucleotide (Silence Select Negative Control Scramble siRANA #4390847,

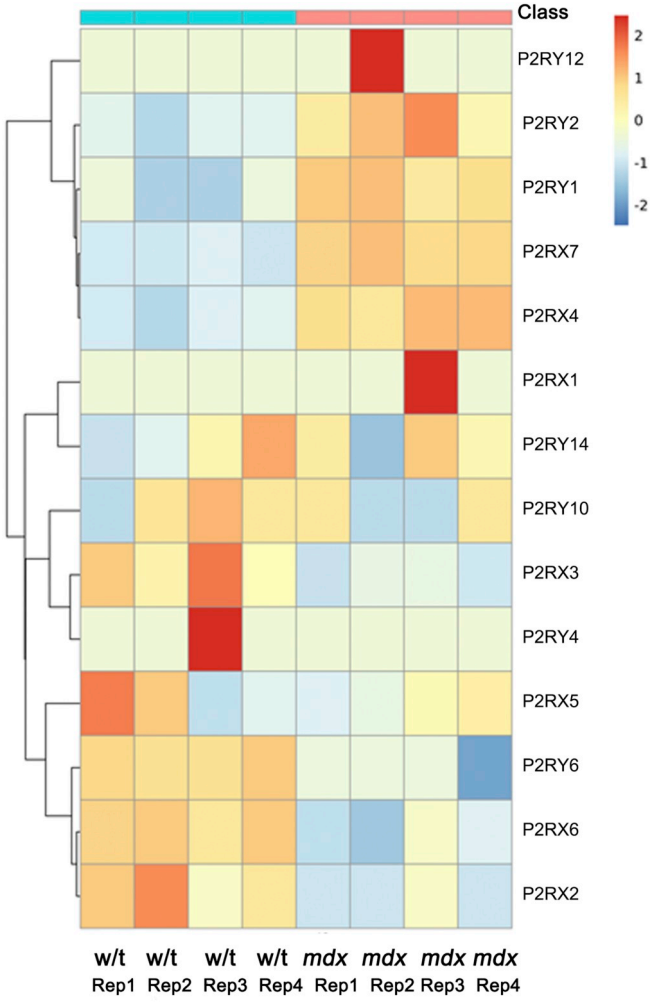

Fig. 2. Heatmap of genes encoding members of the purinoceptor ATP receptor family.
Variance stabilisation transformed read counts were normalised such that each row had mean 0 and standard deviation 1, so that differences between the mdx and w/t cells could be identified, with downregulated genes highlighted blue and upregulated genes highlighted red.

Invitrogen) was used as a negative control. The sequences of P2RY2 siRNA were as follows:

sense sequence 5′-CCGUAAUCCUGGUCUGUUAtt-3′ antisense sequence 3′-UAACAGACCAGGAUUACGGaa-5′.

Mdx and wt myoblasts were transfected with 50 nM siRNA using 3 μl/ml Lipofectamine RNAiMAX (#13778, Invitrogen). The transfection was carried out for 72 h in the medium as described above but without antibiotics and then cells were collected and analysed by Western blotting.

2.6. Isolation of the plasma membrane fraction

For isolation of membrane, around 25 × 106 cells were trypsinised, washed in ice-cold PBS, collected by centrifugation at 200 ×*g* for 3 min and the cell pellet washed again with ice-cold PBS and finally the pellet was resuspend in cold Buffer A included in commercial Plasma Membrane Protein Extraction Kit (101Bio, #P503, Thermo Fisher Scientific). The isolation of the plasma membrane proteins was carried out according to the manufacturer's instruction. The extract plasma membrane proteins were analysed by Western blotting as described above.

2.7. $[Ca^{2+}]_c$ measurements in myoblasts in vitro

Myoblasts were cultured on glass coverslips in a 6-well plate (500,000 cells/well) for 48 h under conditions described above. Cells (70–80% confluent) were loaded with 1 μM Fura 2 AM (Molecular Probes, Oregon) in culture medium for 15 min at 33 °C in a humidified atmosphere of 95% O_2 and 5% CO_2. The cells were then washed twice with the solution composed of 5 mM KCl, 1 mM $MgCl_2$, 0.5 mM Na_2HPO_4, 25 mM HEPES, 130 mM NaCl, 1 mM pyruvate, 5 mM D-glucose, and 0.1 mM $CaCl_2$, pH 7.4 and the coverslips were mounted in a cuvette containing 3 ml of either the nominally Ca^{2+}-free assay solution (as above but 0.1 mM $CaCl_2$ was replaced by 0.05 mM EGTA) or Ca^{2+}-containing assay solution (as above but with 2 mM $CaCl_2$) and maintained at RT in a spectrofluorimeter (Shimadzu, RF5001PC).

Fluorescence was recorded at 510 nm with excitation at 340 and 380 nm. At the end of each experiment the Fura 2 fluorescence was calibrated by addition of 8 μM ionomycin to determine maximal fluorescence followed by addition of EGTA to complete removal of Ca^{2+}.

To compare calcium content in the ER store, w/t and *mdx* myoblasts were treated with ionomycin in the absence of Ca^{2+} in the bath. Ionomycin distributes evenly through cellular membranes, thus an elevation of cytosolic Ca^{2+} concentration is due to a fact that its concentration between the ER and cytosol equilibrates much faster than that between the cytosol and extracellular milieu. It likely mirrors the proportion between surface area of the ER and PM membranes [35]. Though such an approach is not sufficient for calculating Ca^{2+} content in the ER in the absolute units, it is useful to compare a total amount of Ca^{2+} stored in various cells or under different conditions.

Cytosolic Ca^{2+} concentration $[Ca^{2+}]_c$ was calculated according to Grynkiewicz et al. [36]. The cells were treated with 500 μM and 1 mM ATP, 100 μM and 500 μM UTP (both Sigma) and 10 μM AR-C 118925XX (216657-60-2, TOCRIS Bioscience) applied 10 min prior to the addition of ATP and UTP. Each experiment was repeated at least 5 times.

2.8. Immunocytofluorescence (ICC)

Cells were cultured on coverslips (50–60%) in growth medium. After rinsing twice with cold PBS (w/o calcium and magnesium), the myoblasts were fixed in a 4% $^{w}/_{v}$ paraformaldehyde solution (PFA) in PBS for 15 min on ice. Cells were then permeabilized using PBS with 0.1% Triton X-100 for 5 min and blocked in a 5% $^{v}/_{v}$ goat serum (GS, Normal Goat Serum, S-1000, Vector Laboratories IVD) in PBS for 1 h at RT and incubated overnight at 4 °C with primary antibodies (anti-P2RY2 and anti-P2RY4, as described above, diluted 1:100 in blocking buffer). The secondary antibody (diluted 1:1000 in 5% GS in PBS, Alexa Fluor®488 goat anti-Rabbit, Thermo Fisher Scientific) was added for 1 h RT in dark. Then myoblasts were rinsed for 10 min 3 times under agitation between each step of ICC protocol. After staining, cells on coverslips were mounted onto microscope slides sealed in Glycergel Mounting Medium with DAPI (H-1200 VectaShield®, Vector Laboratories) prior to imaging. Images were obtained using a confocal microscope (Zeiss Spinning Disk Confocal Microscope) and image analysis was performed using ImageJ software.

2.9. Random motility assay

15,000 myoblasts (*mdx* and w/t) were seeded into 24-well cell culture plate and grown for 30 h in an appropriate culture medium. Then, multiple different well areas per each cell type were photographed in the bright field or DIC Nomarski contrast using HC PL APO 10x/0.40 Dry objective (Leica Microsystems GmbH) every 15 min for 6 h on inverted DMI6000 microscope (Leica Microsystems GmbH) equipped with DFC350FXR2 CCD camera (Leica Microsystems GmbH) and an environmental chamber (PeCon GmbH). Acquired time-lapse movies were exported to TIFF format and aligned to compensate

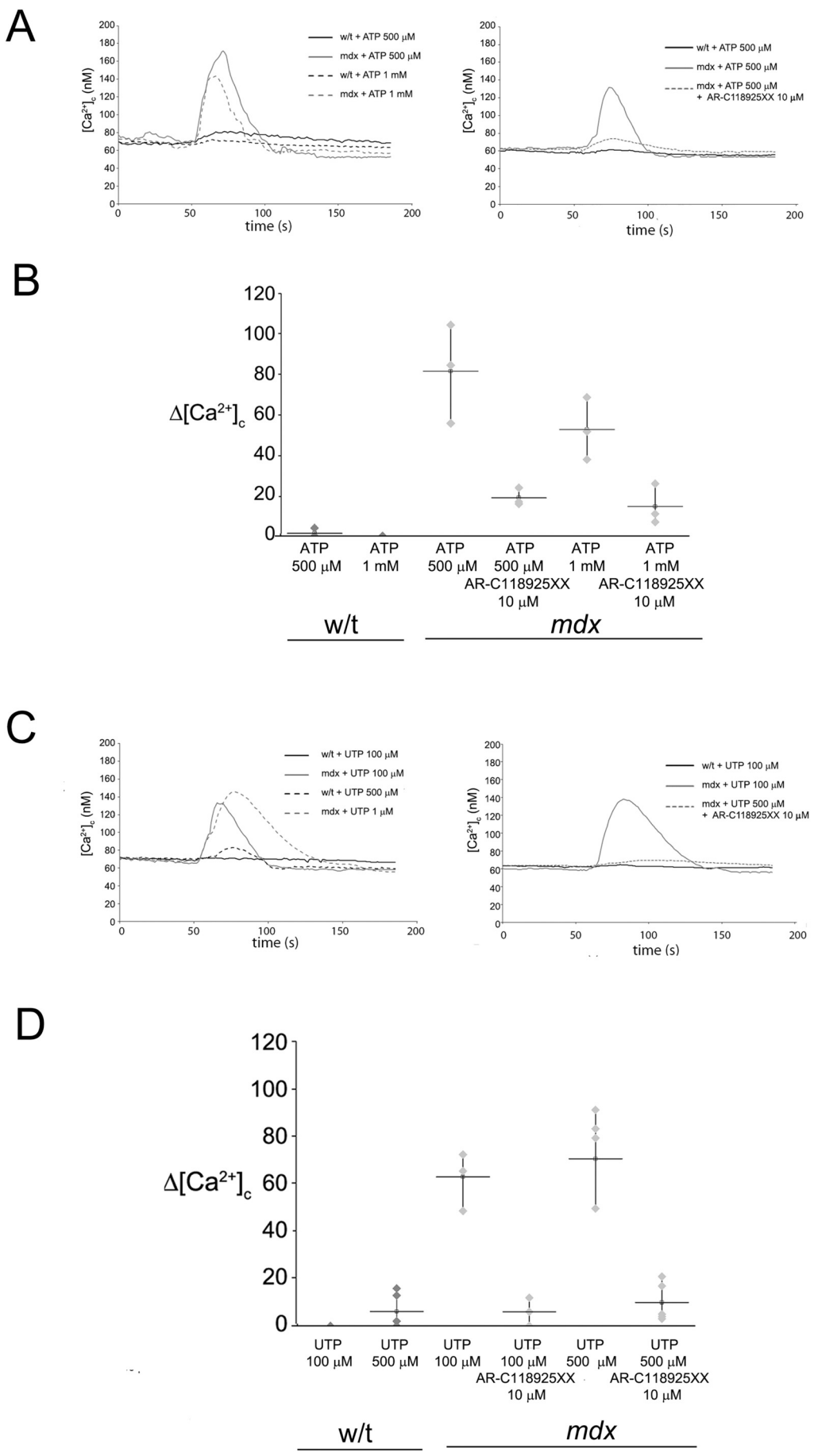

Fig. 3. Effect of ATP, UTP and AR-C118925XX on Ca^{2+} release from the ER stores in myoblasts measured in the absence of extracellular calcium.
A, effect of ATP. Traces from one representative experiment out of three. B, Mean values collected from three experiments ± S.D. C, effect of UTP. Traces from one representative experiment out of five. D, Mean values collected from five experiments ± S.D. Asterisks refer to statistically significant differences, as follows:
mdx vs w/t (500 μM ATP) $*p < 0.029$;
mdx vs w/t (1 mM ATP) $*p < 0.027$;
mdx vs mdx + 10 μM AR-C118925XX (500 μM ATP) $*p < 0.044$;
mdx vs mdx + 10 μM AR-C118925XX (1 mM ATP) $*p < 0.030$;
mdx vs w/t (100 μM UTP) $*p < 0.001$;
mdx vs w/t (500 μM UTP) $*p < 0.001$;
mdx vs mdx + 10 μM AR-C118925XX (100 μM UTP) $*p < 0.0003$
mdx vs mdx + 10 μM AR-C118925XX (500 μM UTP) $*p < 0.001$;
Dark bars – w/t myoblasts, bright bars – mdx myoblasts.

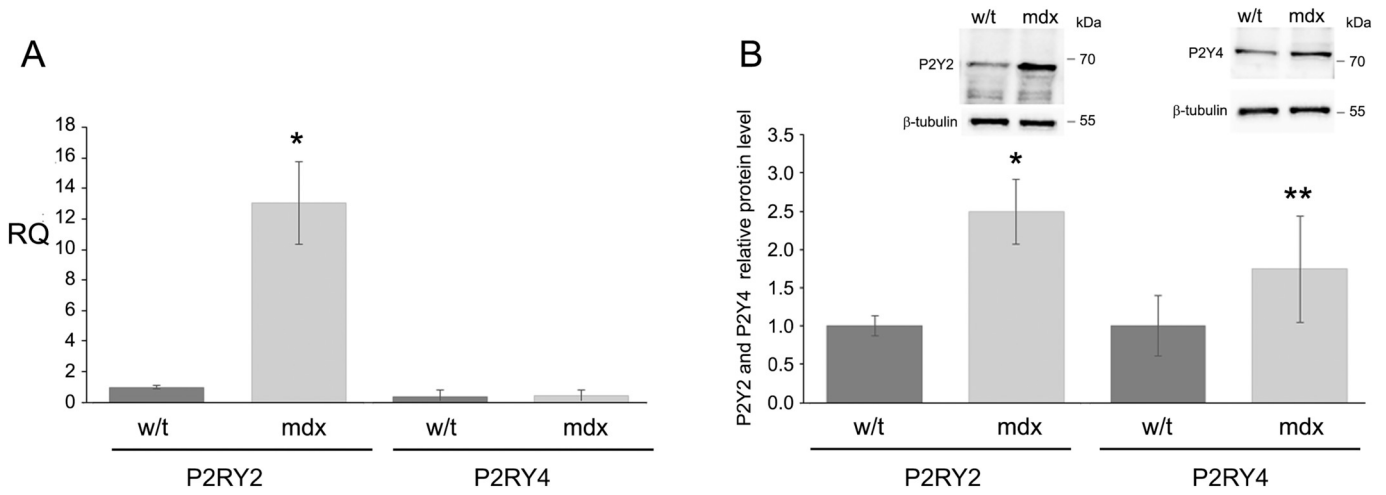

Fig. 4. P2RY2 and P2RY4 expression in w/t and mdx myoblasts.
A, Mean values ± S.D. for qPCR for P2RY2 and P2RY4 transcripts. Data collected from six and four experiments, respectively. *$p < 0.001$. B. Representative Western blots for P2RY2 and P2RY4 and mean values ± S.D. of the relative level of these proteins in mdx myoblasts collected from three and six experiments, respectively. *$p < 0.02$, **$p < 0.05$.

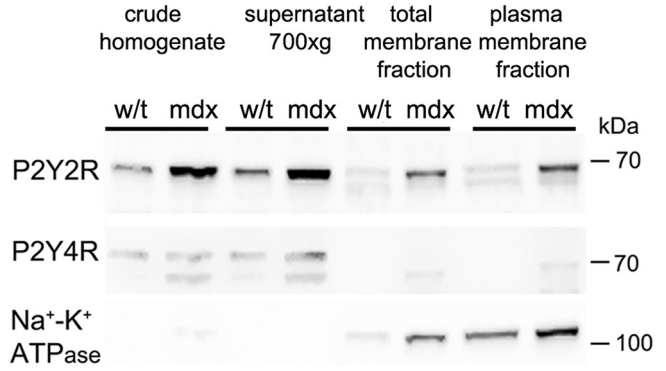

Fig. 5. P2RY2 and P2RY4 localization in the plasma membrane.
Representative Western blot of P2RY2 and P2RY4 in cell fractions grown under "de-immorto" conditions (as in the entire paper) normalised to Na^+-K^+ATPase.

possible drift using an ImageJ plugin. Subsequently, at least 15 cells of each experimental condition were tracked semi-automatically in the time-lapse movies using Track Objects plug-in in Leica MM AF powered by MetaMorph® software (Leica Microsystems GmbH). Cells dividing or colliding with other cells were excluded from the analysis, which has been performed as described below.

2.10. Data analysis

Data are expressed as a mean value ± standard deviation (SD). Statistical significance was assessed by Student's *t*-test A *p* value of < 0.05 was considered statistically significant where $n = 3–5$ for PCR and Western data, and n = 3–9 for other analyses ("n" represents the number of independent experiments with cells derived from different passages). Cell coordinates obtained in the random motility assay were imported into Matlab R2016b software (MathWorks, Inc.) and the movement parameters were calculated using a Matlab script. Each experiment was performed at least five times. Statistical analysis was performed using one way analysis of variance (ANOVA) with the post-hoc all pairwise multiple comparison procedures (Holm-Sidak method).

3. Results

3.1. Transcriptomic analysis of nucleotide receptors

RNASeq analysis was performed as described to identify key transcription alterations between dystrophic (referred to as *mdx*) and wild type (w/t) myogenic immorto cells cultured under the primary myoblast conditions [18,37]. Differential expression analysis revealed a striking global transcriptional change as a result of the *mdx* mutation, with 996 genes upregulated and 1134 genes downregulated in dystrophic myoblasts (Fig. 1A and B). While global differential expression analyses will be presented elsewhere (manuscript in preparation), here we focussed on the purinergic phenotype, which is clearly caused by the *Dmd* gene mutation. In particular, we confirmed significant upregulation of *P2rx7* (4.8-fold increase, $p = 7.39e-40$), which has been previously categorised [15,16]. In addition, we saw significant differential expression, albeit at lower magnitude, for *P2rx4* (1.8-fold increase, $p = 1.16e-16$) and *P2rx6* (1.5-fold decrease, $p = 7.02e-6$). Conversely, no significant differences were seen for *P2rx5* (Fig. 2 $p = 0.62$). Regarding P2RY transcripts, significant differential expression was detected for *P2ry1* (12.8-fold upregulated, $p = 0.006$), *P2ry2* (5.9-fold upregulated, $p = 4.84e-4$), and *P2ry6* (4.8-fold downregulated, $p = 0.02$), although detection of these genes was very low (FPKM < 0.2). *P2ry4* was practically undetectable and showed no change in *mdx* samples.

3.2. Pharmacological and molecular identification of nucleotide receptors

Stimulation with ATP or UTP in the presence of 2 mM $CaCl_2$ in the extracellular milieu resulted in a transient increase in the cytosolic $[Ca^{2+}]$, that was substantially stronger in *mdx* than w/t cells (Suppl. Fig 1.). Under such experimental conditions, $[Ca^{2+}]_c$ peak is a resultant of at least three mechanisms directly responsible for the elevation of cytosolic Ca^{2+} concentration. These include: (i) Ca^{2+} influx through P2RX channels and (ii) store-operated calcium entry (SOCE), which both allow extracellular Ca^{2+} to flow into the cell. Both mechanisms have been identified and analysed by us previously in immortalized and primary w/t and *mdx* myoblasts [15,22]. The third mechanism concerning the eATP-evoked response is Ca^{2+} release from the ER stores due to stimulation of metabotropic nucleotide receptors of the P2RY family. This step is also a prerequisite for SOCE. Moreover, the height and temporal pattern of the $[Ca^{2+}]$c peaks, irrespectively of their

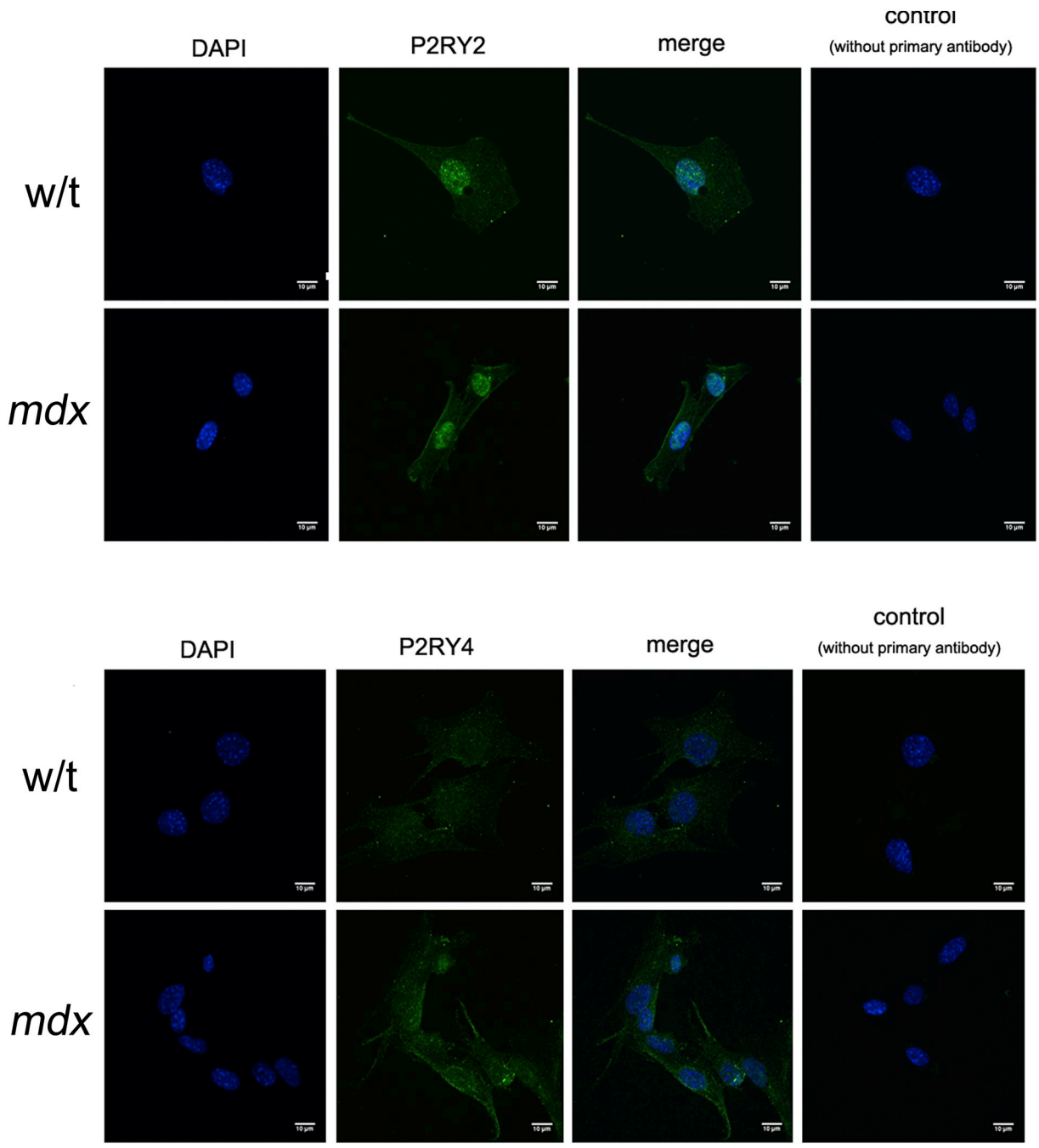

Fig. 6. Immunocytochemical detection of P2RY2 and P2RY4 in w/t and mdx myoblasts.
Upper panel: P2RY2. Increased amount of P2RY2 protein in a cell but particularly in the plasma membrane. Lower panel: P2RY4. Increased total amount of P2RY4 with perinuclear localization. Bar = 10 μM.

origin, are modified by other processes shaping calcium transients in excited cells. To avoid a concomitant stimulation of P2RXs (by ATP) or an activation of the store-operated Ca^{2+} entry following depletion of the ER stores, calcium responses of myoblasts to ATP or UTP were tested under Ca^{2+}-free conditions. Thus, an intensity of calcium release from the ER was first of all considered as a resultant of activities of P2RYs and other proteins involved in the PM–ER signal transduction. Fig. 3 displays a calcium response of w/t and *mdx* myoblasts to ATP (Fig. 3A and B) or UTP (Fig. 3C and D). These agonists stimulate both P2RY2 and P2RY4 but ATP additionally exhibits small affinity to other P2RYs while UTP is particularly specific to P2RY2. Wild type myoblasts were only slightly susceptible to stimulation by ATP or UTP while *mdx* strongly responded to both nucleotides.

Given the differential expression in the RNA seq data, the increased metabotropic response to eATP in dystrophic cells, and also our previous studies, which indicated a P2RY component in the purinergic response in *mdx* cells [15], we performed qPCR and Western blotting analysis of P2RY2 and P2RY4 (the two P2Y receptors responding to eATP) to validate the results from the RNA seq with more sensitive assays. As with the RNAseq data, much higher levels of P2RY2 transcript were found by qPCR in *mdx* compared to w/t myoblasts (Fig. 4), whilst P2RY4 was undetectable by qPCR. Surprisingly however, a band corresponding with the predicted molecular mass of P2RY4 receptor was detected by Western blotting and this band was substantially stronger in *mdx* than in w/t myoblasts (Fig. 4). However, further analysis of plasma membrane proteins revealed that the P2RY2 was

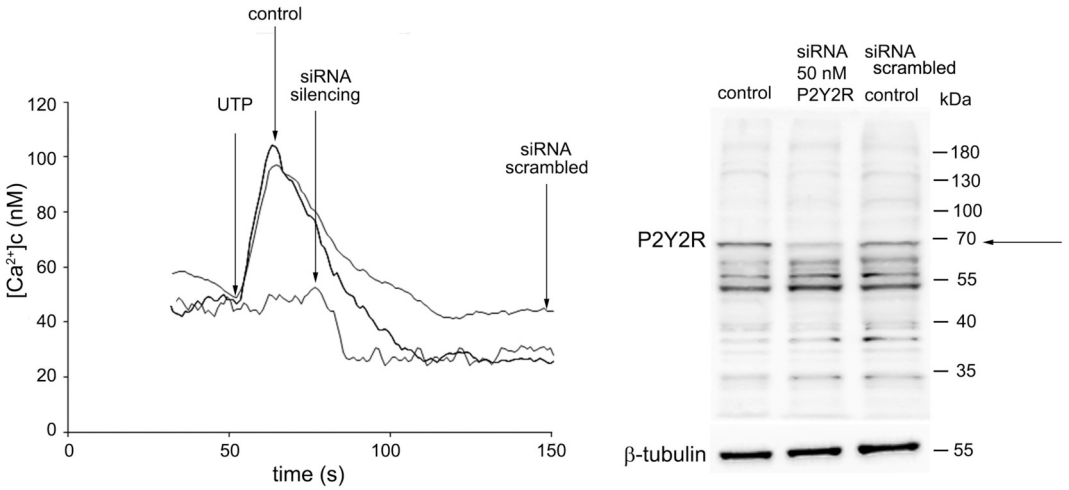

Fig. 7. Effect of P2Y2 gene silencing on UTP-evoked Ca^{2+} release from the ER stores in myoblasts measured in the absence of extracellular calcium. Illustrative Western blot confirming an efficient silencing of the P2RY2 gene and nucleotide–induced Ca^{2+} trace obtained in the same experiment.

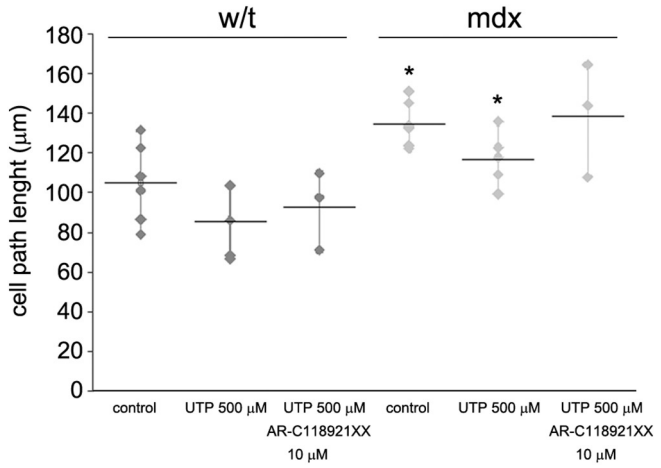

Fig. 8. Effect of UTP and AR-C118925XX on cell motility.
Myoblasts motility (cell path length) expressed in micrometers. Data collected from 5 independent experiments. UTP and AR-C118925XX were used at concentrations of 500 μM and 10 μM, respectively. Each dot corresponds to mean value of speed of motility for 20 individual cells observed in a single experiment. Mdx unstimulated vs w/t unstimulated $p < 0.014$ $n = 5$; mdx stimulated with UTP vs mdx unstimulated $p < 0.044$, $n = 5$.

predominantly found in the membrane fraction and with significantly increased levels in dystrophic myoblasts (Figs. 5 and 6). In contrast, P2RY4 band was present in the cytosol but almost undetectable in the membrane fraction of *mdx* and w/t cells. This cellular localisation made the putative receptor contribution to the extracellular ATP responses unlikely (see Discussion). Immuno-localisation of P2RY2 receptor in myoblasts membrane (Fig. 6) confirmed this conclusion but also revealed a strong signal in the nuclei in addition to cytoplasmic staining.

Indeed, substantially reduced calcium response to ATP or UTP in the presence of a specific P2RY2 antagonist (AR-C118925XX) (see. Fig. 3) confirmed a leading role of P2RY2 in this process. UTP-evoked calcium response is selective and therefore more efficiently blocked by AR-C118925XX. Finally, inhibition of UTP-induced Ca^{2+} release in cells with siRNA silenced P2RY2 expression confirmed calcium response to be P2Y2-evoked (Fig. 7) and allowed us to confirm the specificity of the band detected with anti-P2RY2 antibodies. As shown in Fig. 7, the band of a reduced intensity upon treatment of cells with P2RY2-specific siRNA corresponds to protein of a molecular mass slightly below 70 kDa, which is in agreement with data previously published by Choi et al. [38]. In summary, the qPCR transcript expression data in agreement with increased P2RY2 protein, silencing and pharmacological inhibitor study were all in line with the P2RY2 being responsible for the elevated nucleotide-evoked Ca^{2+} release in dystrophic myoblasts (Fig. 3).

3.3. Functional impact of P2Y receptor activation

Importantly, we also found that the elevated P2RY2 and an increased intensity of calcium response upon stimulation of dystrophic myoblasts with UTP are functionally significant. As shown in Fig. 8, unstimulated dystrophic myoblasts displayed increased overall migration rate. However, stimulation with UTP resulted in reduced migration of these cells. In contrast, the same stimulus had statistically insignificant inhibitory effect on w/t myoblast motility (Fig. 8). Inhibition of this UTP-evoked response in mdx myoblasts by AR-C118925XX, a selective and competitive P2RY2 antagonist, further confirmed the involvement of this receptor.

3.4. Calcium signalling mechanisms leading to increased cytosolic Ca^{2+}

In view of a high complexity of a regulation of intracellular calcium signalling, the increased $[Ca^{2+}]c$ upon stimulation of *mdx* myoblasts with ATP or UTP was unlikely to be explained exclusively by the elevated P2RY2 level in the plasma membrane. Therefore, to gain insight into this mechanism, we have analysed the RNA seq data for possible changes in expression of genes involved in calcium homoeostasis. Gene ontology analysis of genes showing differential expression in the dystrophic cells showed significant enrichment for genes involved in regulation of calcium ion transport into cytosol ($p = 1.54e^{-3}$), whilst global analysis of 870 genes involved in calcium ion transport, binding, and homeostasis functions identified significant modulation (both up and down-regulation) in dystrophic cells (Fig. 9).

To investigate this newly identified abnormality in calcium signalling, we have estimated a relative amount of Ca^{2+} stored in dystrophic and control myoblasts. Moreover, levels of calcium signal transducing proteins linking P2RY2 receptor with the ER calcium stores have been compared. Fig. 10 A shows that a treatment of cells with ionomycin under Ca^{2+}-free conditions resulted in a fast and transient increase of cytosolic Ca^{2+} concentration due to Ca^{2+} release from intercellular stores. Since mitochondrial uncoupling with FCCP did not influence the cytosolic Ca^{2+} concentration (data not shown) it may be assumed that the entire cytosolic Ca^{2+} originates from the ER. A greater increase of cytosolic Ca^{2+} concentrations upon treatment with ionomycin in *mdx*

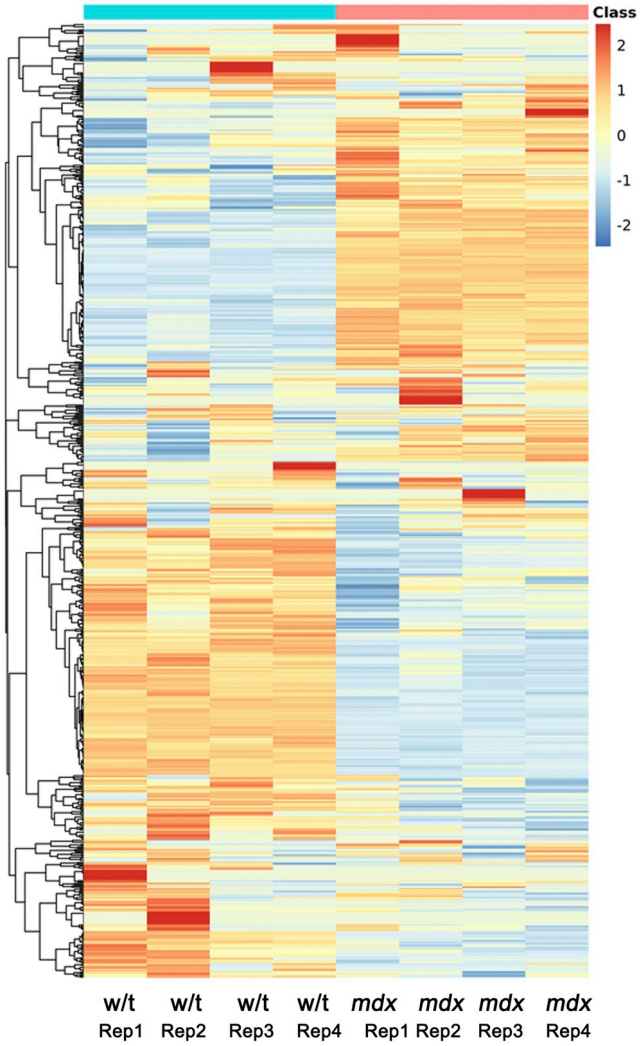

Fig. 9. Heatmap showing expression levels for genes associated with calcium ion homeostasis.
Graph based on gene ontology terms: calcium ion homeostasis (GO:0055074), calcium-mediated signalling (GO:0019722), calcium ion binding (GO:0005509), calcium ion transport (GO:0006816), or calcium channel activity (GO:0005262). Variance stabilisation transformed read counts were normalised such that each row had mean 0 and standard deviation 1, so that differences between the mdx and control (w/t) cells could be identified, with downregulated genes highlighted blue and upregulated genes highlighted red.

myoblasts than in the w/t cells indicates that the former accumulate more Ca^{2+} in the ER. Additionally, *mdx* myoblasts contain more calsequestrin (Fig. 10 B) while the calreticulin level is unaltered by the *mdx* mutation (Fig. 10 C). This finding may suggest higher calcium storage capacity in *mdx* myoblasts and is in line with greater amount of Ca^{2+} released upon treatment of these cells with ionomycin (Fig. 10 A). In addition, substantially elevated levels of SERCA1 and SERCA2B proteins (Fig. 11), which reload ER stores with Ca^{2+}, fit well with the concept of increased abundancy of cellular calcium stores in *mdx* myoblasts.

All results shown hitherto are clearly in line with the elevation of calcium release from the ER upon treatment of cells with ATP or UTP. Therefore, decreased level of Gq_{11} protein (Fig. 12 A) and IP3 receptor (Fig. 12 B), have been unexpected. These proteins mediate P2RY-dependent activation of Ca^{2+} release from the ER, thus their decreased amounts are inconsistent with an assumption suggesting an enhanced signal transduction from P2RY2 to the ER. In contrast, considerably elevated levels of PLCβ isoform 4 (Fig. 13 D), which is responsible for increasing the IP3 concentration, is in line with enhanced Ca^{2+} release and could counterbalance the reduced protein G and IP3R content. To summarize, the significantly stronger calcium response of *mdx* myoblasts treated with ATP or UTP is probably a result of several counteracting changes in specific proteins that were identified in this study.

3.5. Calcium signalling mechanisms leading to restoration of resting $[Ca^{2+}]c$

$[Ca^{2+}]c$ concentration depends on both Ca^{2+} entry into cytosol from the ER and extracellular space and Ca^{2+} extrusion and re-uptake into the ER. As shown in Fig. 14 cellular level of PMCA protein was substantially lower in *mdx* myoblasts than in the w/t cells. This Ca^{2+}-pump exhibits high affinity to Ca^{2+} but it works relatively slowly, thus is thought to be responsible for maintaining low Ca^{2+} concentration in resting cells. On the other hand, an elevated level of sodium-calcium exchangers (NCX1 and 3) suggests an increased efficiency of calcium removal during a recovery phase following cell excitation. This mechanism allows cells to restore resting Ca^{2+} concentration and shapes $[Ca^{2+}]c$ transients. Data shown in Fig. 14 suggest that Ca^{2+} transients due to calcium release from the ER, which were much higher in the *mdx* myoblasts than in their control equivalents, may be attenuated by counteracting processes of Ca^{2+} removal from the cytosol.

Furthermore, to establish the compatibility with the data we previously obtained in *mdx* and *w/t* cells grown under “immorto” conditions we have repeated selected experiments and confirmed the results in such cells (Fig Suppl. 1–6).

4. Discussion

Precise regulation of nucleotide-induced calcium signals is of great importance in stimulated and differentiating satellite cells. It may be accomplished due to concerted activities of numerous “molecular tools” engaged in Ca^{2+} transport, sensing and storage, which are involved in a spatio-temporal controlling of changes in local and global cytosolic $[Ca^{2+}]$. Moreover, excitation of cells via metabotropic receptors needs a contribution of several factors, which form signal-transforming cascades. Purinergic P2Y receptors belong to this category. Available data indicate that the pattern of their expression changes during muscle maturation from satellite cells through myoblasts to fully differentiated muscle fibres [39]. As a proliferation and differentiation of dystrophic myoblast seems to be accelerated in comparison to the w/t cells [13] it is probable that their nucleotide-evoked calcium response may differ [40,41]. Previously, we have shown an increased susceptibility of *mdx* myoblasts to P2RX7-mediated stimulation by ATP. It resulted in an accelerated calcium entry into *mdx* cells and was correlated with an elevated expression of P2RX7 protein [16]. Moreover, prolonged stimulation of *mdx* myoblasts with ATP or, more selectively, with P2RX7-specific agonist BzATP led to the opening of a large pore and additional effects such as stimulated autophagy and MMP-2 release [18,37]. In these cells, as well as in the primary *mdx* myoblasts, an increased level of STIM1 protein seems to be behind significantly increased store-operated calcium entry (SOCE) [22]. In this paper we investigated the first step of cellular response to metabotropic nucleotide receptors stimulation, leading to a depletion of ER stores, which is prerequisite for SOCE activation. This is also the “metabotropic” component to the previously characterized ionotropic ATP response in *mdx* myoblasts [15]. All findings here, together with those published previously [15,22], clearly indicate that calcium signalling in *mdx* myoblasts varies from w/t cells and the amplitude of calcium response is always higher in *mdx* cells. In this study mouse myoblasts were stimulated with ATP or UTP under calcium-free conditions (to avoid any P2X-dependent calcium entry in the case of ATP stimulation) and an activation of the store-operated calcium entry due to depletion of the ER calcium stores. Both agonists may activate P2RY2 and P2RY4. In fact, ATP may weakly

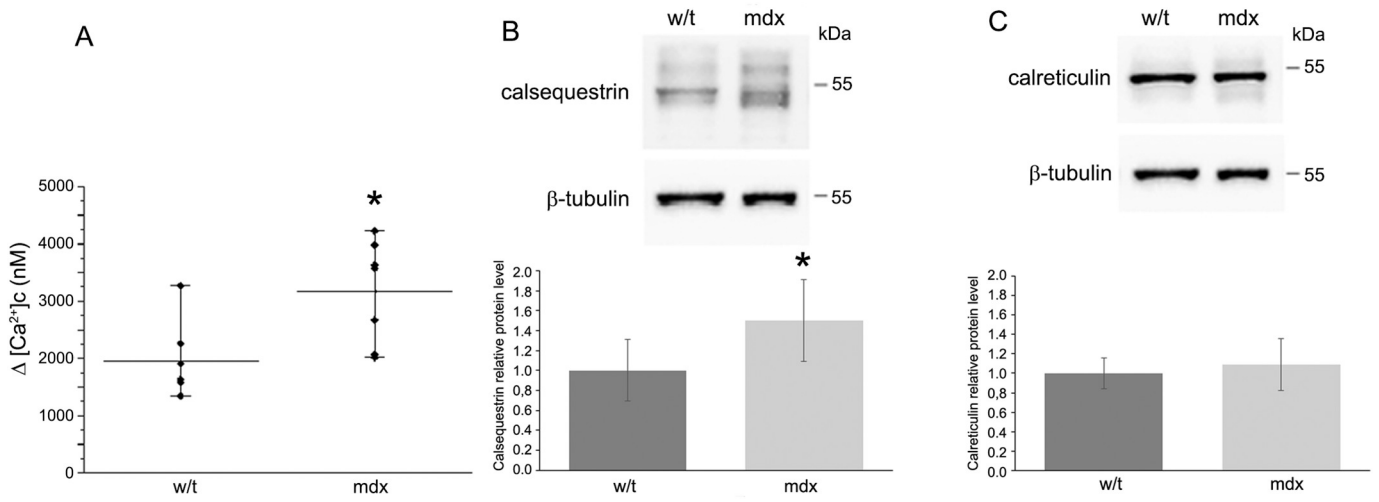

Fig. 10. Relative calcium content in the ER and calsequestrin and calreticulin levels in w/t and mdx myoblasts.
A, Increase of cytosolic Ca^{2+} concentration upon treatment of cells with ionomycin. Mean value of data collected from seven independent experiments ± SD. $^*p < 0.015$.
B, calsequestrin and C, calreticulin content in myoblasts. Representative Western blots and mean values ± S.D. collected from seven experiments. $^*p < 0.020$.

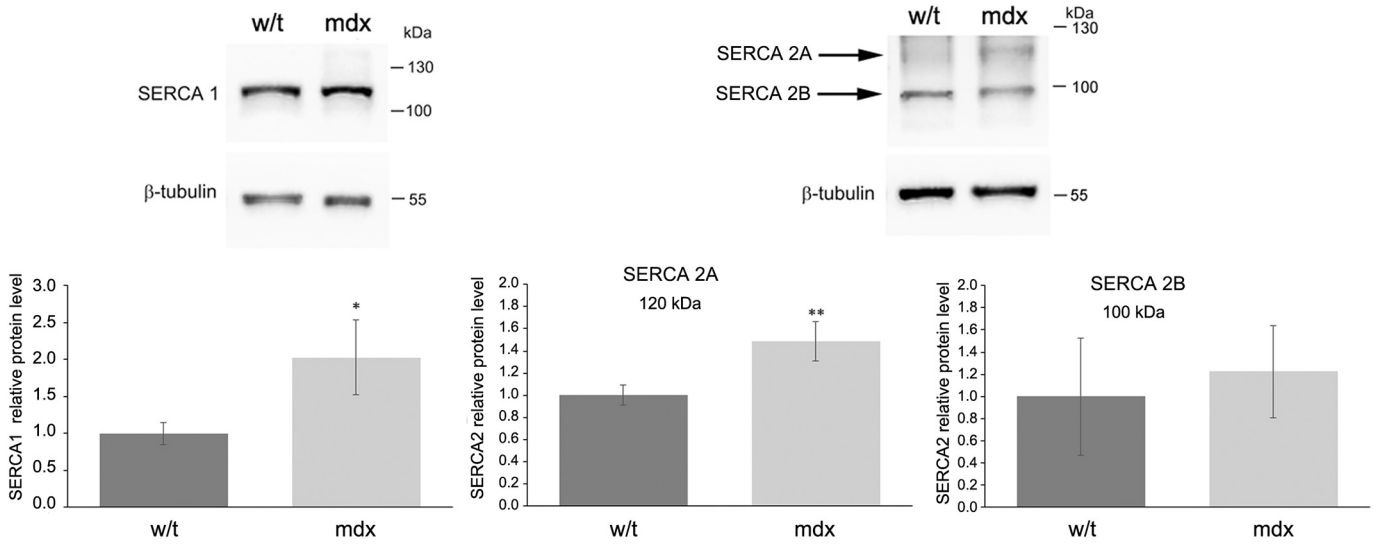

Fig. 11. Relative amounts of SERCA1 and SERCA 2 in w/t and mdx myoblasts. Representative Western blot for SERCA1 and mean values ± S.D. of the relative level of these proteins in mdx myoblasts collected from four experiments. $^*p < 0.022$.Representative Western blot for SERCA2A and mean values ± S.D. of the relative level of these proteins in mdx myoblasts collected from four experiments. $^*p < 0.006$. Representative Western blot for SERCA2B and mean values ± S.D. of the relative level of these proteins in mdx myoblasts collected from four experiments. n.s.

activate some other P2RYs, however considering a particularly high selectivity of this nucleotide for P2RY2 and P2RY4, we focussed on these receptors in further studies. Slightly lower response of cells to 1 mM than to 0.5 mM ATP may be due to additional effects coming from stimulation of other ATP-sensitive proteins putatively leading to a reciprocal inactivation of proteins on the outer surface of the plasma membrane [37]. Discriminating between P2RY2 and P2RY4 activities is difficult because of the lack of satisfactorily specific spectrum of pharmacological tools including agonists and antagonists selective for each of the two types of P2RYs tested. However, a sensitivity of calcium response to P2RY2-specific antagonist and inhibitory effect of silencing the P2RY2 expression indicated that P2RY2 is the predominant receptor activated in *mdx* myoblast treated with ATP under Ca^{2+}-free conditions. P2RY2 gene silencing also confirmed the Western blot band identity as being specific for the P2RY2 protein. It was important because the in-gel mobility of this protein reported by various authors differs significantly [38,42–44].

Moreover, we found that stimulation of dystrophic myoblasts with UTP resulted in significantly reduced migration of these cells (Fig. 8). Inhibition of this effect by AR-C118925XX specific antagonists further confirmed the involvement of P2RY2 receptors. Notably, similar effects of UTP on cell migration were previously shown in leukaemic and nasopharyngeal carcinoma cells [45,46], although an opposite response was also described [47,48]. Given the almost complete lack of *P2ry4* transcripts in RNAseq and qPCR data, finding of an anti-P2RY4 reactive band in the total homogenate of *mdx* myoblasts was unexpected. While the non-specific nature of this band is the simplest explanation, the structure of the *P2ry4* transcript may suggest an interesting alternative explanation. The 3'UTR of mouse *P2ry4* is 3051 bp long and therefore very close to the longest 3'UTR (3354 bp) described for rodents [49]. Interestingly, in a recent study of correlation between gene and protein expression across tissues, genes encoding long 3' UTRs were found in a category of frequently not-detectable at the RNA level but for which protein expression was observed [50]. However, even if genuine, the

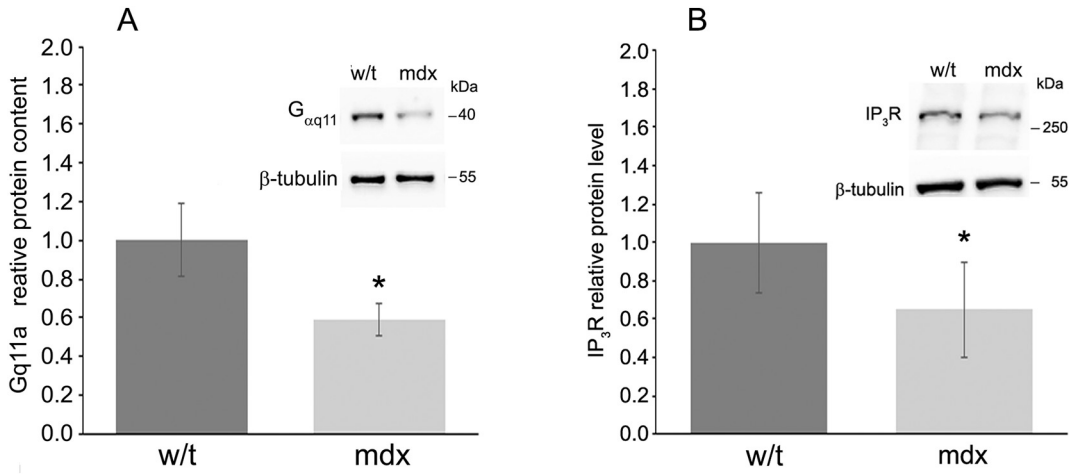

Fig. 12. Relative amount of protein G11q subunit α and IP3R in wt and mdx myoblasts.
A, representative Western blot for Gq_{11} subunit α from one of three independent experiments, and mean values of data collected from three experiments. *$p < 0.047$;
B, representative Western blot for IP3R from one of eight independent experiments, and mean values of data collected from eight experiments. * $p < 0.016$;

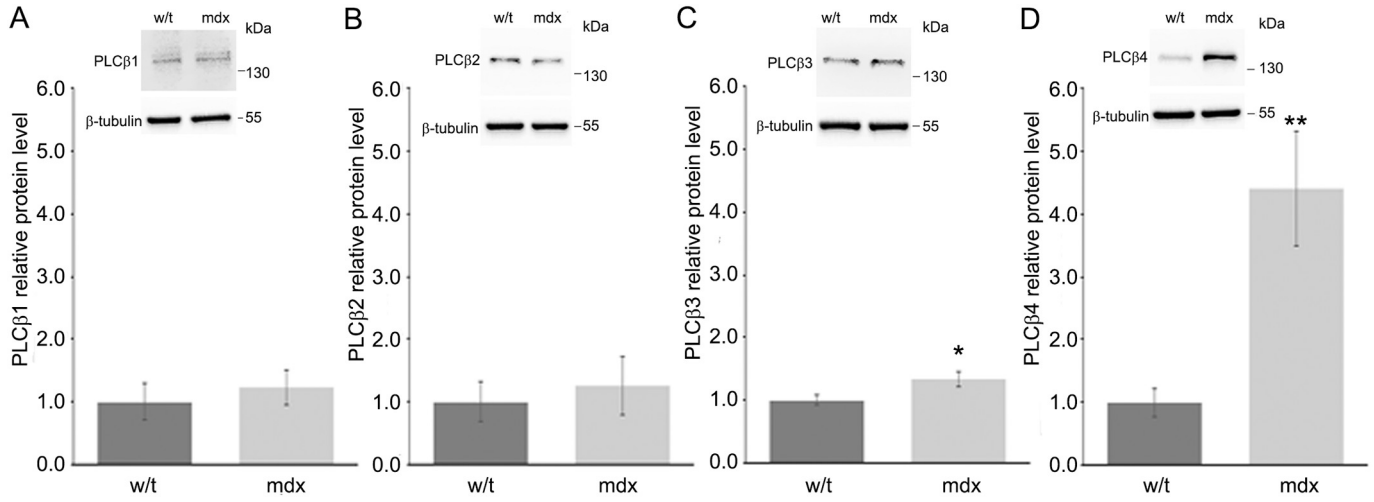

Fig. 13. Relative amount of protein PLC isoforms 1–4 in w/t and mdx myoblasts. Each panel shows one representative Western blot out of four independent experiments and a mean values ± S.D. of collected Western blot data. A, PLCβ1 $n = 4$ $p \leq 0.29$; B, PLCβ2 n = 4 $p \leq 0.552$; C, PLCβ3 n = 4 $p \leq 0.006$; PLCβ4 $n = 3$ $p \leq 0.004$.

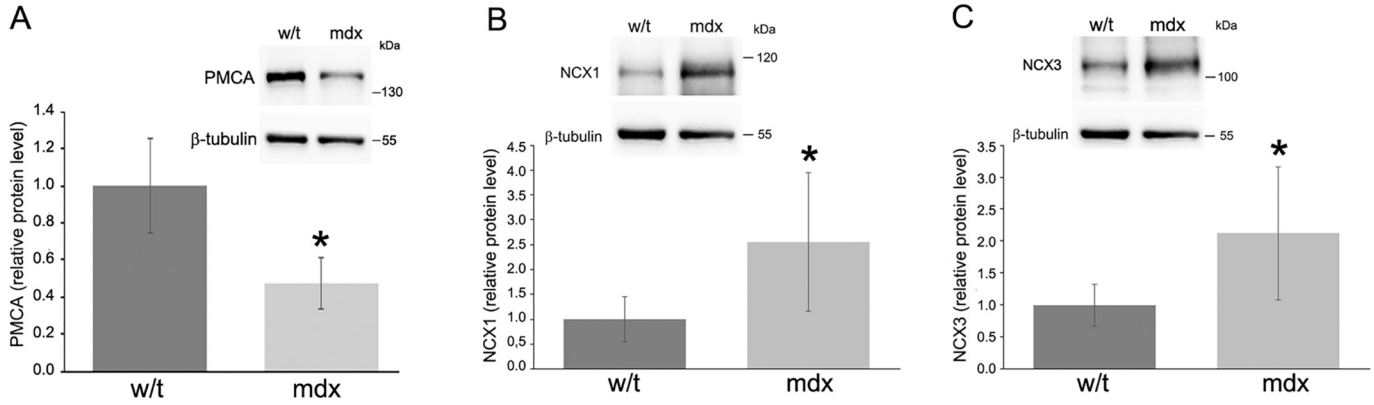

Fig. 14. Relative amount of PMCA protein and NCX isoforms 1 and 3 in w/t and mdx myoblasts.
Each panel shows one representative Western blot out of the number of independent experiments indicated below and a mean values ± S.D. of collected Western blot data. A, PMCA $n = 6$ $p \leq 0.04$; B, NCX1 n = 3 $p \leq 0.046$; C, NCX3 n = 4 $p \leq 0.016$.

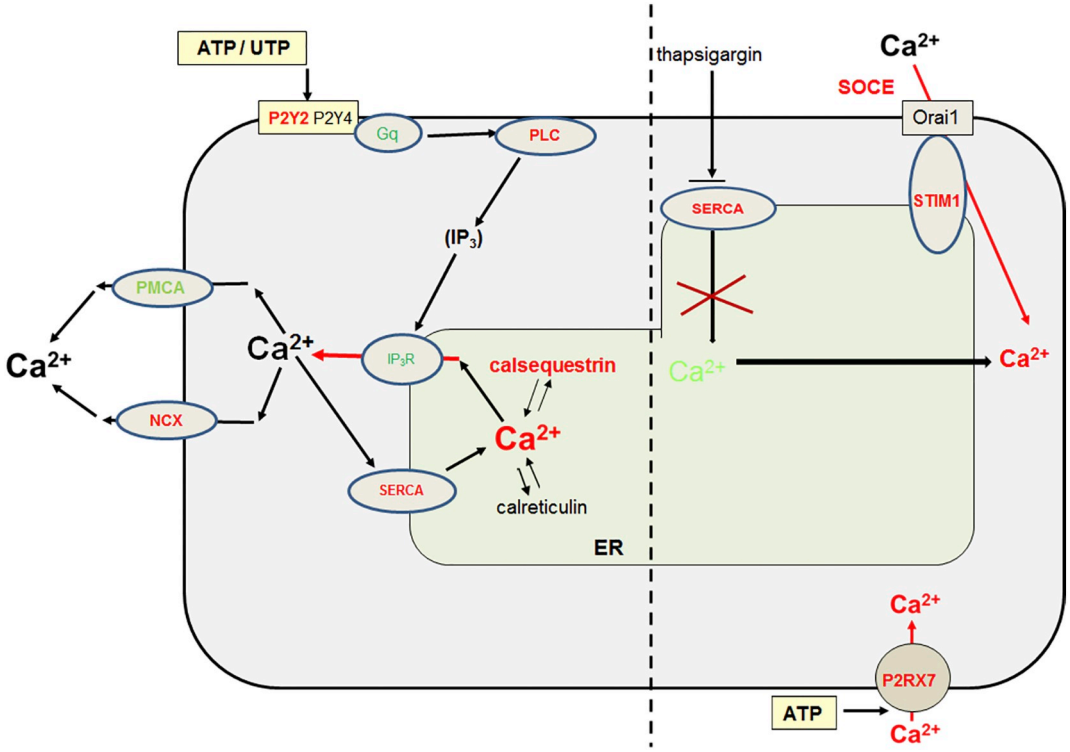

Fig. 15. Diagrammatic summary of the main concepts concerning aberrant calcium homeostasis in mdx myoblasts.
Left site presents data shown in this paper while on the right there are results of previous studies. Red characters or arrows mean increased protein levels or stimulated processes, respectively. Green - decreased proteins levels. Black – unchanged or not determined.

absence of P2RY4 protein in the plasma membrane of cells tested by immunolocalisation or by Western blotting (Suppl. Figs. 4 and 5) excludes its contribution to the purinergic calcium response observed.

The nuclear staining with P2RY2 antibody probably reflects its poor specificity. In fact, Western blot of proteins from isolated nuclei probed with P2RY2 antibodies showed a band corresponding to a much smaller protein, which was insensitive to P2RY2 gene silencing (data not shown).

A functional identification of the P2RY2 as a receptor responsible for ATP/UTP-induced metabotropic calcium response of *mdx* myoblasts together with elevated plasma membrane protein levels suggest a simple cause-effect explanation of increased susceptibility of dystrophic cells to this nucleotide. However, we uncovered a further significant modulation of cellular calcium homeostasis in dystrophic myoblasts.

RNASeq and biochemical data shown here indicate a set of changes, which may affect calcium signalling in *mdx* myoblasts. They include alterations in signal-transducing processes down-stream from the plasma membrane receptors. Subtle interplay between “on and off” mechanisms leads to a balanced elevation of calcium responses, which fulfil the cellular demand. Final intensity of the calcium signal is a resultant of many, sometimes opposite, regulatory processes. Such a complex regulation prevents cell overloading with calcium. Increased levels of P2RY2 and PLC proteins as well as the over-abundance of the ER calcium stores may explain the increased Ca^{2+} release from the ER. Potentially, the latter could give a misguided impression of an elevated P2RY2 activity or, at least, result in overestimation of its contribution to the intensity of calcium responses. On the other hand, substantially reduced level of Gq11 subunit α and IP3R counteract the elevated signal transduction. It seems possible that the type of receptor decides the specificity of cellular response while its intensity might be further regulated by a very broad toolkit composed of proteins involved in calcium signalling. Special attention should also be paid to proteins involved in the restoration of the resting cytosolic Ca^{2+} concentration: NCX, SERCA and PMCA, as they are directly involved in regulating/shaping calcium signals regardless of a mechanism behind the induction of cellular calcium response. Thus, P2RY2 stimulation activates a signal transduction cascade, which may contribute to a regulation of the intensity of calcium response to the metabotropic receptors stimuli. It is noteworthy that similar effect of *mdx* mutation on NCX1 and SERCA 1 and 2 was previously found in myoblasts grown under immortalizing conditions [22]. Results shown here complement the general picture describing differences in the pattern of molecular tools (channels, pumps, exchangers, buffers) responsible for Ca^{2+} homeostasis in w/t and *mdx* myoblasts. An overview in Fig. 15 summarizes data shown here and in two previous publications [15,22]. We propose that *mdx* mutation affects the balance between particular processes engaged in the intracellular calcium signalling. This may reflect a cellular adaptation mechanism allowing myoblasts to precisely control intensity of responses to purinergic stimuli and maintain Ca^{2+} homeostasis without affecting cell viability. Results presented in this paper are in line with the hypothesis that phenotypic effects of *mdx* mutation occur as early as in undifferentiated muscle cells. Expression of full-length dystrophin transcripts in muscles is developmentally regulated: Proliferating myoblasts do not have detectable levels of dystrophin protein, while it is found in myotubes/myofibres. This observation, understandably, led to the commonly accepted hypothesis that dystrophin mutations have an impact in differentiated muscles only. As a result, research into the mutant phenotype has focused on the absence of dystrophin in myofibres sarcolemma. In contrast to this established belief, some well-documented experimental data indicate multiple phenotypic changes in undifferentiated mutant cells [for. rev. see Fig. 5]. Although the molecular mechanism behind these broad spectrum changes of $[Ca^{2+}]c$ regulation caused by *mdx* mutation is still elusive, data shown here strengthen a hypothesis of a very early (in terms of muscle cell differentiation) onset of DMD. It sheds new light on DMD pathophysiology and potentially might be important for pharmacological alleviation of DMD symptoms, as an alternative to largely ineffective attempts at restoration of dystrophin in muscle cells, which

in view of our findings, seems to be a late intervention [5]. We also demonstrated that these changes are due to *Dmd* gene mutation and not caused by cell immortalisation or being evoked by the effects of the dystrophic niche on primary myoblasts because these abnormalities are present in immortalized and de-immortalized cells alike. However, the results shown here should be confirmed in primary cells, similarly to what was done in previous studies [22]. Finally, it is important to stress that the data presented here reflect changes in undifferentiated dystrophic muscle cells and it is not easy to extrapolate these findings to fully matured myofibres. Muscle differentiation produces substantial reorganization of calcium signalling as electrically non-excitable cells become excitable ones. It involves an increased role of voltage-gated Ca^{2+} channels and an increased ability of the sarcoplasmic reticulum to maintain a high level of calcium stored and released upon plasma membrane depolarization. It may explain the increased content of calsequestrin in myofibres in comparison to myoblasts [51,52]. Nevertheless, DMD affects calcium homeostasis in both cell types. While some changes observed in myoblasts seem to persist in matured muscle fibres [16,22,53] other may disappear [39]. Moreover, muscle differentiation results in metabolic specialisation and differences between fast and slow fibres will also play a role. Therefore, it is hard to conclude whether myoblast abnormalities described here can contribute to the differential phenotype of specific muscles in DMD without direct analyses in both cell types.

5. Conclusion

The *mdx* myoblasts exhibit elevated P2RY2 stimulation. Receptor overexpression determines the selectivity of cell responses while the intensity of the calcium signal appears dependent on the modulation of a set of proteins responsible for intracellular signal transduction, Ca^{2+} transport and storage. Thus, the resultant Ca^{2+} response reflects activity of processes increasing $[Ca^{2+}]_c$, which are counterbalanced by mechanism preventing calcium overload.

Diverse responses of w/t and *mdx* myoblasts to ATP or UTP and significant differences in RNASeq profiles confirm the hypothesis that phenotypic effects of *Dmd* mutation occur as early as in undifferentiated muscle cells.

Supplementary data to this article can be found online at https://doi.org/10.1016/j.bbadis.2019.01.002.

Transparency document

The Transparency document associated with this article can be found, in online version.

Acknowledgements

This work was supported by the National Science Centre, Poland, accordingly to the decision number DEC-2013/11/B/NZ3/01573 and the Polish Ministry of National Defense, Poland, project “Kościuszko” no: 523/2017/DA. The research was performed in part in the Multimodal Laboratory of Cell Adhesion and Motility, part of NanoFun laboratory co-financed by the European Regional Development Fund within the Innovation Economy Operational Programme POIG.02.02.00-00-025/09.

References

[1] N. Doorenweerd, A. Mahfouz, M. van Putten, R. Kaliyaperumal, P.A.C. T'Hoen, J.G.M. Hendriksen, A.M. Aartsma-Rus, J.J.G.M. Verschuuren, E.H. Niks, M.J.T. Reinders, H.E. Kan, B.P.F. Lelieveldt, Timing and localization of human dystrophin isoform expression provide insights into the cognitive phenotype of Duchenne muscular dystrophy, Sci. Rep. 7 (2017), https://doi.org/10.1038/s41598-017-12981-5PMCID: PMC5626779PMID: 28974727.

[2] J. Ehmsen, E. Poon, K. Davies, The dystrophin-associated protein complex, J. Cell Sci. 115 (2002) 2801–2803.

[3] S.M.M. Ghahraman, I.R. Graham, T. Athanasopoulos, C. Trollet, M. Pohlschmidt, M.R. Crompton, G. Dickson, RNAi-mediated knockdown of dystrophin expression in adult mice does not lead to overt muscular dystrophy pathology, Hum. Mol. Genet. 17 (2008) 2622–2632.

[4] E.P. Rader, R. Turk, T. Willer, D. Beltrán, K-i. Inamori, T.A. Peterson, J. Engle, S. Prouty, K. Matsumura, F. Saito, M.E. Anderson, K.P. Campbell, Role of dystroglycan in limiting contraction-induced injury to the sarcomeric cytoskeleton of mature skeletal muscle, Proc. Natl. Acad. Sci. U. S. A. 113 (2016) 10992–10997.

[5] D.C. Górecki, Dystrophin: the dead calm of a dogma, Rare Dis. 4 (2016) e1153777, , https://doi.org/10.1080/21675511.2016.1153777.

[6] D. Merrick, L.K. Stadler, D. Larner, J. Smith, Muscular dystrophy begins early in embryonic development deriving from stem cell loss and disrupted skeletal muscle formation, Dis. Model. Mech. 2 (2009) 374–388.

[7] A. Sacco, F. Mourkioti, R. Tran, J. Choi, M. Lewellyn, P. Kraft, M. Shkreli, S. Delp, J.H. Pomerantz, S.E. Artandi, H.M. Blau, Short telomeres and stem cell exhaustion model Duchenne muscular dystrophy in mdx/mTR mice, Cell 143 (2010) 1059–1071.

[8] F. Mourkioti, J. Kustan, P. Kraft, J.W. Day, M.M. Zhao, M. Kost-Alimova, A. Protopopov, R.A. DePinho, D. Bernstein, A.K. Meeker, H.M. Blau, Role of telomere dysfunction in cardiac failure in Duchenne muscular dystrophy, Nat. Cell Biol. 15 (2013) 895–904.

[9] N.A. Dumont, Y.X. Wang, J. von Maltzahn, A. Pasut, C.F. Bentzinger, C.E. Brun, M.A. Rudnicki, Dystrophin expression in muscle stem cells regulates their polarity and asymmetric division, Nat. Med. 21 (2015) 1455–1463.

[10] N.C. Chang, M.-C. Sincennes, F.P. Chevalier, C.E. Brun, M. Lacaria, J. Segalés, P. Muñoz-Cánoves, H. Ming, M.A. Rudnicki, The dystrophin glycoprotein complex regulates the epigenetic activation of muscle stem cell commitment, cell, Stem Cells 22 (2018) 755–768, https://doi.org/10.1016/j.stem.2018.03.022.

[11] G. Jasmin, C. Tautu, M. Vanasse, P. Brochu, R. Simoneau, Impaired muscle differentiation in explant cultures of Duchenne muscular dystrophy, Lab. Investig. 50 (1984) 197–207.

[12] B. Lucas-Heron, J.M. Mussini, B. Ollivier, Is there a maturation defect related to calcium in muscle mitochondria from dystrophic mice and Duchenne and Becker muscular dystrophy patients, J. Neurol. Sci. 90 (1989) 299–306.

[13] Z. Yablonka-Reuveni, J.E. Anderson, Satellite cells from dystrophic (mdx) mice display accelerated differentiation in primary cultures and in isolated myofibers, Dev. Dyn. 235 (2006) 203–212, https://doi.org/10.1002/dvdy.20602.

[14] M. Onopiuk, W. Brutkowski, K. Wierzbicka, S. Wojciechowska, J. Szczepanowska, J. Fronk, H. Lochmüller, D.C. Górecki, K. Zabłocki, Mutation in dystrophin-encoding gene affects energy metabolism in mouse myoblasts, Biochem. Biophys. Res. Commun. 386 (2009) 463–466.

[15] D. Yeung, K. Zabłocki, C.-F. Lien, T. Jiang, S. Arkle, W. Brutkowski, J. Brown, H. Lochmuller, J. Simon, E.A. Barnard, D.C. Górecki, Increased susceptibility to ATP via alteration of P2X receptor function in dystrophic mdx mouse muscle cells, FASEB J. 20 (2006) 610–620.

[16] C. Young, W. Brutkowski, C.-F. Lien, S. Arkle, H. Lochmüller, K. Zabłocki, D.C. Górecki, P2X7 purinoceptor alterations in dystrophic mdx mouse muscles: relationship to pathology and potential target for treatment, J. Cell. Mol. Med. 16 (2012) 1026–1037.

[17] D. Ferrari, M. Munerati, L. Melchiorri, S.F. Hanau, O.R. Baricordi Di Virgilio, Responses to extracellular ATP of lyphoblastoid cell lines from Duchenne muscular dystrophy patients, Am. J. Phys. 267 (1994) C886–C892.

[18] C.N. Young, A. Sinadinos, A. Lefebvre, P. Chan, S. Arkle, D. Vaudry, D.C. Gorecki, A novel mechanism of autophagic cell death in dystrophic muscle regulated by P2RX7 receptor large-pore formation and HSP90, Autophagy 11 (2015) 113–130.

[19] A. Sinadinos, C.N. Young, R. Al-Khalidi, A. Teti, P. Kalinski, S. Mohamad, L. Floriot, T. Henry, G. Tozzi, T. Jiang, O. Wurtz, A. Lefebvre, M. Shugay, J. Tong, D. Vaudry, S. Arkle, J.C. doRego, D.C. Górecki, sP2RX7 purinoceptor: a therapeutic target for ameliorating the symptoms of duchenne muscular dystrophy, PLoS Med. 12 (10) (2015) e1001888.

[20] E. Gazzerro, S. Baldassari, S. Assereto, F. Fruscione, A. Pistorio, C. Panicucci, S. Volpi, L. Perruzza, C. Fiorillo, C. Minetti, E. Traggiai, F. Grassi, C. Bruno, Enhancement of muscle T regulatory cells and improvement of muscular dystrophic process in mdx mice by blockade of extracellular ATP/P2X axis, Am. J. Pathol. 185 (2015) 3349–3360.

[21] R. Al-Khalidi, C. Panicucci, P. Cox, N. Chira, J. Róg, C.N.J. Young, R.E. McGeehan, K. Ambati, J. Ambati, K. Zabłocki, E. Gazzerro, S. Arkle, C. Bruno, D.C. Górecki, Zidovudine ameliorates pathology in the mouse model of Duchenne muscular dystrophy via P2RX7 purinoceptor antagonism, Acta Neuropathol. Commun. 6 (2018) 27, https://doi.org/10.1186/s40478-018-0530-4.

[22] M. Onopiuk, W. Brutkowski, C. Young, E. Krasowska, J. Róg, M. Ritso, S. Wojciechowska, S. Arkle, K. Zabłocki, D.C. Górecki, Store-operated calcium entry contributes to abnormal Ca^{2+} signaling in dystrophic mdx mouse myoblasts, Arch. Biochem. Biophys. 569 (2015) 1–9.

[23] J.E. Morgan, J.R. Beauchamp, C.N. Pagel, M. Peckham, P. Ataliotis, P.S. Jat, M.D. Noble, K. Farmer, T.A. Patridge, Myogenic cell lines derived from transgenic moce carrying a thermolabile T antigen: a model system for the derivation of tissue-specific and mutation-specific cell lines, Dev. Biol. 162 (1994) 486–498.

[24] C. Brun, D. Suter, C. Pauli, P. Dunant, H. Lochmüller J.M. Burgunder, D. Schümperli, J. Weis, U7 snRNAs induce correction of mutated dystrophin pre-mRNA by exon skipping, Cell. Mol. Life Sci. 60 (2003) 557–566.

[25] L.H. Jørgensen, N. Larochelle, K. Orlopp, P. Dunant, R.W. Dudley, R. Stucka, C. Thirion, M.C. Walter, S.H. Laval, H. Lochmuller, Efficient and fast functional screening of microdystrophin constructs in vivo and in vitro for therapy of Duchenne muscular dystrophy, Hum. Gene Ther. 20 (2009) 641–650.

[26] A. Musarò, L. Barberi, Isolation and culture of mouse satellite cells, Methods Mol.

Biol. 633 (2010) 101–111, https://doi.org/10.1007/978-1-59745-019-5_8.
[27] S. Andrews, FastQC: A Quality Control Tool for High Throughput Sequence Data, http://www.bioinformatics.babraham.ac.uk/projects/fastqc, (2010).
[28] F. Krueger, Trim Galore! A Quality Trimming Tool for High Throughput Sequence Data, https://www.bioinformatics.babraham.ac.uk/projects/trim_galore/, (2012).
[29] A. Dobin, C.A. Davis, F. Schlesinger, J. Drenkow, C. Zaleski, S. Jha, P. Batut, M. Chaisson, T.R. Gingeras, STAR: ultrafast universal RNA-seq aligner, Bioinformatics 29 (2013) 15–21.
[30] M.I. Love, W. Huber, S. Anders, Moderated estimation of fold change and dispersion for RNA-seq data with DESeq2, Genome Biol. 15 (2014) 550, https://doi.org/10.1186/s13059-014-0550-8].
[31] R Core Team, R: A Language and Environment for Statistical Computing, R Foundation for Statistical Computing, Vienna, Austria, 2017https://www.R-project.org/.
[32] M. Lawrence, W. Huber, H. Pagès, P. Aboyoun, M. Carlson, R. Gentleman, M.T. Morgan, V.J. Carey, Software for computing and annotating genomic ranges, PLoS Comput. Biol. 9 (2013) e1003118.
[33] Y. Benjamini, Y. Hochberg, Controlling the false discovery rate: a practical and powerful approach to multiple testing, J. R. Stat. Soc. Ser. B Methodol. 57 (1995) 289–300 www.jstor.org/stable/2346101 (JSTOR).
[34] G. Yu, L.G. Wang, Y. Han, Q.Y. He, clusterProfiler: an R package for comparing biological themes among gene clusters, OMICS 16 (2012) 284–287, https://doi.org/10.1089/omi.2011.0118.
[35] Y.V. Evtodienko, V.V. Teplova, J. Duszyński, L. Wojtczak, Effect of cyclosporin A on Ca^{2+} fluxes and the rate of respiration in Ehrlich ascites tumour cells, Biochem. Mol. Biol. Int. 35 (1995) 1113–1121.
[36] G. Grynkiewicz, M. Poenie, R.Y. Tsien, A new generation of Ca^{2+} indicators with greatly improved fluorescence properties, J. Biol. Chem. 260 (1985) 3440–3450.
[37] C.N.J. Young, N. Chira, J. Róg, R. Al-Khalidi, M. Benard, L. Galas, P. Chan, D. Vaudry, K. Zabłocki, D.C. Górecki, Sustained activation of P2X7 induces MMP-2-evoked cleavage and functional purinoceptor inhibition, J. Mol. Cell Biol. 10 (2018) 229–242, https://doi.org/10.1093/jmcb/mjx030.
[38] R.C. Choi, G.K. Chu, N.L. Siow, A.W. Yung, L.Y. Yung, P.S. Lee, C.C. Lo, J. Simon, T.T. Dong, E.A. Barnard, K.W. Tsim, Activation of UTP-sensitive P2Y2 receptor induces the expression of cholinergic genes in cultured cortical neurons: a signaling cascade triggered by Ca^{2+} mobilization and extracellular regulated kinase phosphorylation, Mol. Pharm. 84 (2013) 50–61, https://doi.org/10.1124/mol.112.084160.
[39] G. Burnstock, T.R. Arnett, I.R. Orriss, Purinergic signalling in the musculoskeletal system, Purinergic Signal 9 (2013) 541–572, https://doi.org/10.1007/s11302-013-9381-4.
[40] W. Banachewicz, D. Supłat, P. Krzemiński, P. Pomorski, J. Barańska, P2 nucleotide receptors on C2C12 satellite cells, Purinergic Signal 1 (2005) 249–257, https://doi.org/10.1007/s11302-005-6311-0.
[41] R. Araya, M.A. Riquelme, E. Brandan, J.C. Sáez, The formation of skeletal muscle myotubes requires functional membrane receptors activated by extracellular ATP, Brain Res. Brain Res. Rev. 47 (2004) 174–188.
[42] L. Wang, M. Andersson, L. Karlsson, M.-A. Watson, D.J. Cousens, S. Jern, D. Erlinge, Increased mitogenic and decreased contractile P2 receptors in smooth muscle cells by shear stress in human vessels with intact endothelium, Arterioscler. Thromb. Vasc. Biol. 23 (2003) 1370–1376.
[43] G. Nylund, L. Hultman, S. Nordgren, D.S. Delbro, P2Y2- and P2Y4 purinergic receptors are over-expressed in human colon cancer, Auton. Autacoid Pharmacol. 27 (2007) 79–84.
[44] F.G. Vázquez-Cuevas, E.P. Zárate-Díaz, E. Garay, R.O. Arellano, Functional expression and intracellular signalling of UTP-sensitive P2Y receptors in theca-interstitial cells, Reprod. Biol. Endocrinol. 88 (2010), https://doi.org/10.1186/1477-7827-8-88.
[45] V. Salvestrini, R. Zini, L. Rossi, S. Gulinelli, R. Manfredini, E. Bianchi, W. Piacibello, L. Caione, G. Migliardi, M.R. Ricciardi, A. Tafuri, M. Romano, S. Salati, F. Di Virgilio, S. Ferrari, M. Baccarani, D. Ferrari, R.M. Lemoli, Purinergic signaling inhibits human acute myeloblastic leukemia cell proliferation, migration, and engraftment in immunodeficient mice, Blood 119 (2012) 217–226, https://doi.org/10.1182/blood-2011-07-370775.
[46] G. Yang, S. Zhang, Y. Zhang, Q. Zhou, S. Peng, T. Zhang, C. Yang, Z. Zhu, F. Zhang, The inhibitory effects of extracellular ATP on the growth of nasopharyngeal carcinoma cells via P2Y2 receptor and osteopontin, J. Exp. Clin. Cancer Res. 33 (2014), https://doi.org/10.1186/1756-9966-33-53 http://www.jeccr.com/content/33/1/53.
[47] A. Lamarca, A. Gella, T. Martiañez, M. Segura, J. Figueiro-Silva, C. Grijota-Martinez, R. Trullas, N. Casals, Uridine 5′-triphosphate promotes in vitro Schwannoma cell migration through matrix metalloproteinase-2 activation, PLoS One 9 (2014) e98998, , https://doi.org/10.1371/journal.pone.0098998.
[48] G.A. Weisman, M. Wang, Q. Kong, N.E. Chorna, J.T. Neary, G.Y. Sun, F.A. González, C.I. Seye, L. Erb, Molecular determinants of P2Y2 nucleotide receptor function: implications for proliferative and inflammatory pathways in astrocytes, Mol. Neurobiol. 31 (2005) 169–183.
[49] F. Mignone, C. Gissi, S. Liuni, G. Pesole, Untranslated regions of mRNAs, Genome Biol. 3 (2002), http://genomebiology.com/2002/3/3/reviews/0004.
[50] I. Kosti, N. Jain, D. Aran, A.J. Butte, M. Sirota, Cross-tissue analysis of gene and protein expression in normal and cancer tissues, Sci. Rep. 6 (2016), https://doi.org/10.1038/srep24799.
[51] S. Tharin, P.A. Hamel, E.M. Conway, M. Michalak, M. Opas, Regulation of calcium binding proteins calreticulin and calsequestrin during differentiation in the myogenic cell line L6, J. Cell. Physiol. 166 (1996) 547–560.
[52] J.W. Park, J.H. Lee, S.W. Kim, J.S. Han, K.S. Kang, S.J. Kim, T.S. Park, Muscle differentiation induced up-regulation of calcium-related gene expression in quail myoblasts, Asian Australas. J. Anim. Sci. 31 (2018) 1507–1515, https://doi.org/10.5713/ajas.18.0302.
[53] J.N. Edwards, O. Friedrich, T.R. Cully, F. von Wegner, R.M. Murphy, B.S. Launikonis, Upregulation of store-operated Ca^{2+} entry in dystrophic mdx mouse muscle, Am. J. Phys. Cell Phys. 299 (2010) C42–C50, https://doi.org/10.1152/ajpcell.00524.2009.